JACS
JOURNAL OF THE AMERICAN CHEMICAL SOCIETY

Subscriber access provided by American Chemical Society

Article

Electron Inventory, Kinetic Assignment (E), Structure, and Bonding of Nitrogenase Turnover Intermediates with CH and CO

Hong-In Lee, Morten Srlie, Jason Christiansen, Tran-Chin Yang, Junlong Shao, Dennis R. Dean, Brian J. Hales, and Brian M. Hoffman

J. Am. Chem. Soc., **2005**, 127 (45), 15880-15890• DOI: 10.1021/ja054078x • Publication Date (Web): 19 October 2005

Downloaded from http://pubs.acs.org on March 25, 2009

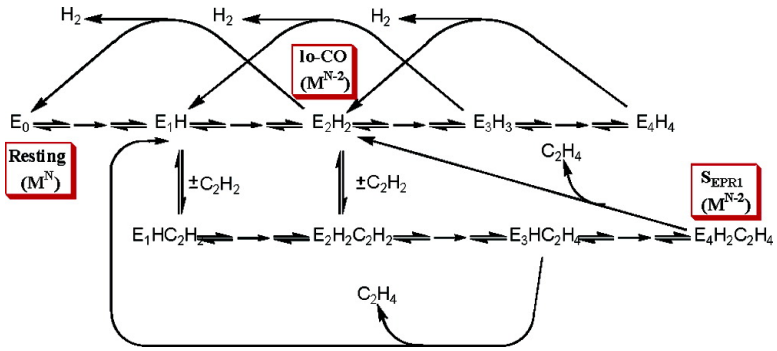

More About This Article

Additional resources and features associated with this article are available within the HTML version:

- Supporting Information
- Links to the 6 articles that cite this article, as of the time of this article download
- Access to high resolution figures
- Links to articles and content related to this article
- Copyright permission to reproduce figures and/or text from this article

View the Full Text HTML

ACS Publications
High quality. High impact.

Journal of the American Chemical Society is published by the American Chemical Society. 1155 Sixteenth Street N.W., Washington, DC 20036

J|A|C|S
ARTICLES
Published on Web 10/19/2005

Electron Inventory, Kinetic Assignment (E_n), Structure, and Bonding of Nitrogenase Turnover Intermediates with C_2H_2 and CO

Hong-In Lee,*,† Morten Sørlie,§ Jason Christiansen,‡ Tran-Chin Yang,|| Junlong Shao,|| Dennis R. Dean,*,‡ Brian J. Hales,*,§ and Brian M. Hoffman*,||

Contribution from the Department of Chemistry Education, Kyungpook National University, Daegu, 702-701, Korea, Department of Biochemistry, Virginia Tech, Blacksburg, Virginia 24061, Department of Chemistry, Louisiana State University, Baton Rouge, Louisiana 70803, and Department of Chemistry, Northwestern University, Evanston, Illinois 60208

Received June 20, 2005; E-mail: bmh@northwestern.edu; bhales@lsu.edu; deandr@vt.edu; leehi@knu.ac.kr

Abstract: Improved ^{1}H ENDOR data from the S_{EPR1} intermediate formed during turnover of the nitrogenase α-195^{Gln} MoFe protein with $C_2^{1,2}H_2$ in $^{1,2}H_2O$ buffers, taken in context with the recent study of the intermediate formed from propargyl alcohol, indicate that S_{EPR1} is a product complex, likely with C_2H_4 bound as a ferracycle to a single Fe of the FeMo-cofactor active site. 35 GHz CW and Mims pulsed ^{57}Fe ENDOR of ^{57}Fe-enriched S_{EPR1} cofactor indicates that it exhibits the same valencies as those of the CO-bound cofactor of the lo-CO intermediate formed during turnover with CO, [Mo^{4+}, Fe^{3+}, Fe_6^{2+}, $S_9^{2-}(d^{43})]^{+1}$, reduced by $m = 2$ electrons relative to the resting-state cofactor. Consideration of ^{57}Fe hyperfine coupling in S_{EPR1} and lo-CO leads to a picture in which CO bridges two Fe of lo-CO, while the C_2H_4 of S_{EPR1} binds to one of these. To correlate these and other intermediates with Lowe−Thorneley (LT) kinetic schemes for substrate reduction, we introduce the concept of an "electron inventory". It partitions the number of electrons a MoFe protein intermediate has accepted from the Fe protein (n) into the number transmitted to the substrate (s), the number that remain on the intermediate cofactor (m), and the additional number delivered to the cofactor from the P clusters (p): $n = m + s - p$ (with $p = 0$ here). The cofactors of lo-CO and S_{EPR1} both are reduced by $m = 2$ electrons, but the intermediates are not at the same LT reduction stage (E_n): ($n = 2$; $m = 2$, $s = 0$) for lo-CO; ($n = 4$; $s = 2$, $m = 2$) for S_{EPR1}. This is the first proposed correlation of an LT E_n kinetic state with a well-defined chemical state of the enzyme.

Introduction

Nitrogenase is a two-protein system that reduces dinitrogen to ammonia: $N_2 + 8H^+ + 8e^- + 16MgATP \rightarrow 2NH_3 + H_2 + 16MgADP + 16Pi$. ATP hydrolysis drives electron transfer from the nitrogenase Fe protein to the MoFe protein, which contains the active site. The MoFe protein contains the [8Fe−7S] cluster (P-cluster), which mediates electron flow, and the $S = {}^3/_2$ iron-molybenum cofactor cluster (FeMo-co; [Mo,Fe_7,S_9-homocitrate]), which binds and reduces substrate.[1] X-ray crystallographic studies of nitrogenases from *Azotobactor vinelandii* (*Av*), *Klebsiella pneumoniae* (*Kp*), and *Clostridium pasteurianium* (*Cp*) have revealed the structures of all three proteins in great detail.[2−6] The FeMo-cofactor can be viewed as two metal cubanes (Mo3Fe3S and 4Fe3S) linked by three μ-2 sulfides, with an N, O, or C atom (denoted **X**), at the center of the cofactor, Figure 1;[7] we have presented evidence that **X** is not a nitrogen.[8,9] Despite the detailed structural information, major questions remain regarding where and how substrates and reaction intermediates bind to and react on the cofactor, and about the electronic states of the cofactor that are involved.

It has long been known that when the MoFe protein is incubated with CO under turnover conditions, the $S = {}^3/_2$ electron paramagnetic resonance (EPR) signal of the resting state disappears and two new $S = {}^1/_2$ signals appear: one under low pressure of CO (lo-CO; 0.08 atm) and the other under high pressure of CO (hi-CO; 0.5 atm).[10−15] In recent years, a number

† Kyungpook National University.
‡ Virginia Tech.
§ Louisiana State University.
|| Northwestern University.

(1) Howard, J. B.; Rees, D. C. *Chem. Rev.* **1996**, *96*, 2965−2982.
(2) Kim, J.; Rees, D. C. *Nature* **1992**, *360*, 553−560.
(3) Kim, J.; Rees, D. C. *Science* **1992**, *257*, 1677−1682.
(4) Chan, M. K.; Kim, J.; Rees, D. C. *Science* **1993**, *260*, 792−794.
(5) Kim, J.; Woo, D.; Rees, D. C. *Biochemistry* **1993**, *32*, 7104−7115.
(6) Mayer, S. M.; Lawson, D. M.; Gormal, C. A.; Roe, S. M.; Smith, B. E. *J. Mol. Biol.* **1999**, *292*, 871−891.
(7) Einsle, O.; Tezcan, F. A.; Andrade, S. L. A.; Schmid, B.; Yoshida, M.; Howard, J. B.; Rees, D. C. *Science (Washington, DC, United States)* **2002**, *297*, 1696−1700.
(8) Lee, H.-I.; Benton, P. M. C.; Laryukhin, M.; Igarashi, R. Y.; Dean, D. R.; Seefeldt, L. C.; Hoffman, B. M. *J. Am. Chem. Soc.* **2003**, *125*, 5604−5605.
(9) Yang, T.-C.; Maeser, N. K.; Laryukhin, M.; Lee, H.-I.; Dean, D. R.; Seefeldt, L. C.; Hoffman, B. M. *J. Am. Chem. Soc.* **2005**, *127*, 12804−12805.
(10) Lowe, D. J.; Eady, R. R.; Thorneley, R. N. F. *Biochem. J.* **1978**, *173*, 277−290.
(11) Davis, L. C.; Henzl, M. T.; Burris, R. H.; Orme-Johnson, W. H. *Biochemistry* **1979**, *18*, 4860−4869.

10.1021/ja054078x CCC: $30.25 **© 2005 American Chemical Society**

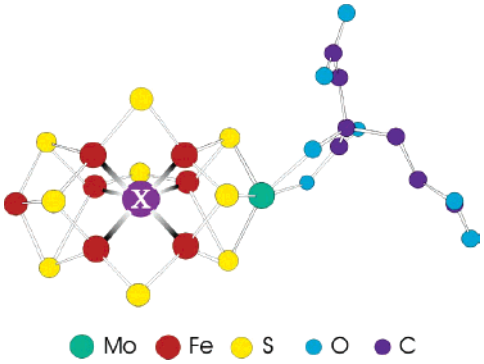

Figure 1. Structure of the FeMo-cofactor of the nitrogenase MoFe protein. Species "X" indicates an unidentified light element,[7] which is not a nitrogen.[9]

of intermediates have been trapped during substrate reduction. During the reduction of CS_2 by wild-type (WT) enzyme, three new $S = {}^1/_2$ signals sequentially appear and disappear.[16] When WT nitrogenase turns over under C_2H_2, the $S = {}^3/_2$ resting-state EPR signal diminishes, but no new signal is observed, whereas when the α-195^{Gln} MoFe protein (*Av*) is incubated with C_2H_2 under turnover conditions, three new $S = {}^1/_2$ EPR signals replace the resting-state signal, S_{EPR1} with $\mathbf{g} = [2.123, 1.978, 1.949]$ and two others.[15,17,18] More recently, a number of $S = {}^1/_2$ intermediate states of the MoFe protein and its mutants have been trapped during turnover of α-70 MoFe variants (*Av*) with different substrates: propargyl alcohol (α-70^{Ala}),[19,20] protons (α-70^{Ile}),[21] and hydrazine.[22] All these turnover states have been studied by ^{1,2}H, ^{13}C, and ^{14,15}N electron-nuclear double resonance (ENDOR) spectroscopy, as appropriate. Such studies identify the inhibitor/substrate/reduction products bound to the turnover-state FeMo-cofactors and provide detailed structural information about their binding modes. In addition, ^{57}Fe ENDOR spectroscopy was used to prove the signals from CO-intermediates indeed arise from the cofactor, and not the P cluster, and to investigate the valency of lo- and hi-CO.[13,23]

In the present study we use Q-band (35 GHz) continuous wave (CW) and Mims pulsed ^{1,2}H ENDOR to reexamine the structure of the C_2H_2-derived species bound to the S_{EPR1} cofactor. Our initial study[18] suggested that S_{EPR1} contains a *reactant* complex of C_2H_2 bound to the cofactor so as to bridge

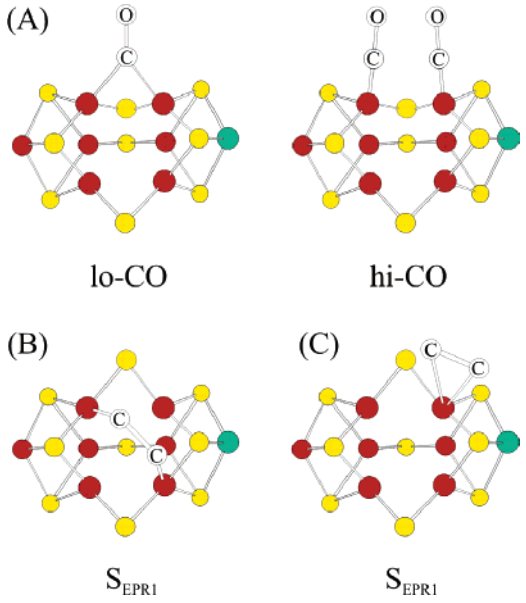

Figure 2. (A) Previously suggested binding modes of CO to the FeMo-cofactor in lo-CO and hi-CO state wild-type MoFe proteins.[14] (B) Previously suggested binding mode of C_2H_2 to the FeMo-cofactor in S_{EPR1} state α-195^{Gln} MoFe protein.[18] (C) Alternative binding mode of C_2H_2 to the FeMo-cofactor in S_{EPR1} state α-195^{Gln} MoFe protein, including the ferracycle suggested by the propargyl alcohol intermediate.[19] Species "X" is removed in the figures for simplicity.

two diagonal Fe ions of a four-Fe "face" of the cofactor (Figure 2B). This restudy is prompted by our recent finding that the intermediate trapped during turnover of the α-70^{Ala} mutant with the alkyne, propargyl alcohol (PA), is a complex of the alkene *product*, allyl alcohol, bound to a single Fe ion as a ferracycle, Figure 2C.[19,20] Indeed, improved ^{1}H ENDOR data from S_{EPR1} now discloses that it too is a *product* complex and, thus, likely to have C_2H_4 bound to a single Fe of the cofactor as a ferracycle.

We also use 35 GHz CW and Mims pulsed ^{57}Fe ENDOR to examine the Fe ions of the cofactor in its S_{EPR1} ($S = {}^1/_2$) state trapped during turnover of the isotopically ^{57}Fe-enriched α-195^{Gln} MoFe protein with C_2H_2 and compare the present finding with those of the lo-CO state trapped during turnover with CO.[23] Crystallographic study of the α-195^{Gln} MoFe protein reveals that the structure of the protein is essentially identical to that of the wild-type MoFe protein.[17] Furthermore, the wild-type and α-195^{Gln} MoFe proteins have identical K_m's for the reduction of C_2H_2 to C_2H_4 and the reduction of C_2H_4 to C_2H_6, and neither protein generates any detectable C_2H_6 during C_2H_2 reduction.[24,25] Therefore, the ^{57}Fe ENDOR data obtained from the lo-CO state of the wild-type FeMo-cofactor can be compared directly to that of S_{EPR1} for the α-195^{Gln} MoFe protein. We earlier inferred that CO binds to the lo-CO cofactor by bridging two Fe ions (Figure 2A).[14] Direct comparison of the ^{57}Fe ENDOR results for the two intermediates suggests that C_2H_4 binds to one of these two Fe ions.

The ^{57}Fe ENDOR measurements also can be analyzed in terms of the valencies of the metal ions in the turnover intermediates. In our earlier ^{57}Fe ENDOR studies of the CO-inhibited, lo-CO, MoFe protein (*Av1*) state, we argued that there are *only* two plausible valency assignments for the [Fe$_7$, S$_9$, Mo]^q

(12) Pollock, R. C.; Lee, H.-I.; Cameron, L. M.; DeRose, V. J.; Hales, B. J.; Orme-Johnson, W. H.; Hoffman, B. M. *J. Am. Chem. Soc.* **1995**, *117*, 8686−8687.
(13) Christie, P. D.; Lee, H.-I.; Cameron, L. M.; Hales, B. J.; Orme-Johnson, W. H.; Hoffman, B. M. *J. Am. Chem. Soc.* **1996**, *118*, 8707−8709.
(14) Lee, H.-I.; Cameron, L. M.; Hales, B. J.; Hoffman, B. M. *J. Am. Chem. Soc.* **1997**, *119*, 10121−10126.
(15) Lee, H.-I.; Cameron, L. M.; Christiansen, J.; Christie, P. D.; Pollock, R. C.; Song, R.; Sorlie, M.; Orme-Johnson, W. H.; Dean, D. R.; Hales, B. J.; Hoffman, B. M. *ACS Symp. Ser.* **2003**, *858*, 150−178.
(16) Ryle, M. J.; Lee, H.-I.; Seefeldt, L. C.; Hoffman, B. M. *Biochemistry* **2000**, *39*, 1114−1119.
(17) Sorlie, M.; Christiansen, J.; Lemon, B. J.; Peters, J. W.; Dean, D. R.; Hales, B. J. *Biochemistry* **2001**, *40*, 1540−1549.
(18) Lee, H.-I.; Sorlie, M.; Christiansen, J.; Song, R.; Dean, D. R.; Hales, B. J.; Hoffman, B. M. *J. Am. Chem. Soc.* **2000**, *122*, 5582−5587.
(19) Lee, H.-I.; Igarashi, R. Y.; Laryukhin, M.; Doan, P. E.; Dos Santos, P. C.; Dean, D. R.; Seefeldt, L. C.; Hoffman, B. M. *J. Am. Chem. Soc.* **2004**, *126*, 9563−9569.
(20) Dos Santos, P. C.; Igarashi, R. Y.; Lee, H.-I.; Hoffman, B. M.; Seefeldt, L. C.; Dean, D. R. *Acc. Chem. Res.* **2005**, *38*, 208−214.
(21) Igarashi, R. Y.; Laryukhin, M.; Santos, P. C. D.; Lee, H.-I.; Dean, D. R.; Seefeldt, L. C.; Hoffman, B. M. *J. Am. Chem. Soc.* **2005**, *127*, 6231−6241.
(22) Barney, B. M.; Laryukhin, M.; Igarashi, R. Y.; Lee, H.-I.; Santos, P. C. D.; Yang, T.-C.; Hoffman, B. M.; Dean, D. R.; Seefeldt, L. C. *Biochemistry* **2005**, *44*, 8030−8037.
(23) Lee, H.-I.; Hales, B. J.; Hoffman, B. M. *J. Am. Chem. Soc.* **1997**, *119*, 11395−11400.
(24) Kim, C.-H.; Newton, W. E.; Dean, D. R. *Biochemistry* **1995**, *34*, 2798−2808.
(25) Fisher, K.; Dilworth, M. J.; Kim, C.-H.; Newton, W. E. *Biochemistry* **2000**, *39*, 2970−2979.

cluster of lo-CO: $q = +1$, with a d^{43} electron count, and $q = +3$ with d^{41}.[23] We further proposed that the proper choice for lo-CO was $q = +1$, with the FeMo-cofactor described as $[Mo^{4+}, Fe^{3+}{}_1, Fe^{2+}{}_6, S^{2-}{}_9]^{+}(d^{43})$. The ^{57}Fe ENDOR results presented here indicate that the cofactors of lo-CO and S_{EPR1} share a common electronic state, with the previously proposed valencies and (d^{43}) electron count. Our earlier study had, however, advanced indirect arguments which suggested the valence states of resting-state and CO-inhibited cofactors to be the same,[23] while subsequent Mössbauer experiments[26] and DFT computations[27] on the resting-state MoFe protein (*Av1*) suggested that the resting-state cofactor has the electronic state $[Mo^{4+}, Fe^{3+}{}_3, Fe^{2+}{}_4, S^{2-}{}_9]^{3+}$ (d^{41}). Smith and co-workers[28] subsequently explained that both direct assignments are correct and that the cofactor state shared by the intermediates is reduced by two electrons relative to the resting state ($m = 2$).

Once the structure of its substrate-derived species and the reduction level (m) and metal-ion valencies of the FeMo-co have been characterized, the next step must be the correlation of the intermediate with the nitrogenase catalytic mechanism, beginning with its placement within a Lowe−Thorneley (LT) kinetic scheme for nitrogenase catalysis.[29−31] LT kinetic schemes denote MoFe protein turnover intermediates as E_n, where n is the number of electrons (and protons) that have been delivered to the resting MoFe protein.[32] However, in a typical intermediate, the cluster does not retain all n electrons delivered to it: some of these are "passed on" to reduce the substrate. The most significant advance of this report is the development of a formalism to correlate intermediates with kinetic states. We introduce the concept of an "electron inventory", which relates the number of electrons a MoFe protein intermediate has accepted from the Fe protein (n), which specifies an LT E_n kinetic intermediate, to the number that have been transmitted to the substrate (s), the number that reside on the cofactor (m), and the number delivered to the cofactor from the P clusters (p): $n = m + s - p$ (with $p = 0$ here). We show that the electron inventory of a nitrogenase turnover intermediate can be determined by combining ENDOR data with results from studies of catalysis. In the context of this formalism we conclude that lo-CO and S_{EPR1} have cofactors at the same stage of reduction (m) but are not in the same E_n state. The value of n for S_{EPR1} is correlated with the bonding within the product complex, and its determination allows us to infer whether the alkene product of alkyne reduction is acting as a dative π donor or forms a σ-bonded ferracyclopropane. These assignments of lo-CO and S_{EPR1} are the first complete characterization of the reduction state of both the FeMo-cofactor and substrate of a turnover intermediate, and this is the first time that an E_n state has been correlated with a well-defined chemical state of the enzyme.

Materials and Methods

Cell Growth and Protein Purification: The α-195^{Gln} MoFe protein was purified from *Azotobacter vinelandii* strain DJ997. Cells were grown at 30 °C with pressurized sparging (80 L/min at 5 psi) and 125 rpm agitation in a 150-L custom-built fermenter (W. B. Moore, Inc. Easton, PA) in modified Burk medium containing 10 mM urea as a the sole nitrogen source. After reaching a density of 220 Klett units (red filter), the cells were derepressed for *nif* gene expression by concentration (6-fold) using a custom-built AG Technologies tangential-flow concentrator and resuspended in Burk medium with no added nitrogen source. All protein manipulations were performed under anaerobic conditions maintained using either a Schlenk apparatus or an anaerobic glovebox. The α-195^{Gln} MoFe protein was purified using a combination of immobilized metal-affinity chromatography (IMAC) and DEAE-Sepharose anion exchange chromatography as previously described.[33] Protein was quantified using a modified biuret assay with bovine serum albumin as the standard, and purity was monitored by SDS-PAGE electrophoresis. For 360 g of wet-weight cells, purification yielded approximately 1.1 g of purified α-195^{Gln} MoFe protein. Nitrogenase assays were performed as previously described,[24] and activities for the α-195^{Gln} MoFe protein used in the current work were similar to those previously reported.[24] To generate the MoFe protein enriched with ^{57}Fe, strain DJ997 was grown on medium as described above but containing 10mM ^{57}Fe (94.7%, Advanced Materials, Inc., Great Neck, NY).

Turnover EPR Samples: Turnover samples consisted of 20 μM Fe protein, 100 μM α-195^{Gln} MoFe protein, 0.1 atm of C_2H_2, 10 mM ATP, 25 mM $MgCl_2$, 20 mM $Na_2S_2O_4$, and 50 mM TES−KOH pH 7.4. Prior to turnover, the above mixture (without the Fe protein) was preincubated for 20 min at 30 °C with 0.1 atm of C_2H_2 under 1.0 atm of Ar. After initiation of turnover by the addition of Fe protein, a 100-μL sample was transferred to a Q-band ENDOR tube where it was rapidly frozen in liquid N_2. The interval between turnover initiation and final freezing was approximately 2 min.

Mass Spectrometry and FTIR Samples: Turnover samples (1.0 mL) consisted of 75 μM Fe protein, 292 μM α-195^{Gln} MoFe protein, 20 mM ATP, 30 mM creatine phosphate, 0.125 mg creatine phosphokinase, 50 mM $MgCl_2$, 40 mM $Na_2S_2O_4$, and 100 mM TES−KOH pH 7.4 in a 7.5-mL septum-covered bottle. Prior to turnover, the above mixture (without the Fe protein) was preincubated for 20 min at 30 °C with 1.0 atm of either 1.0 atm of C_2H_4 (BOC) using D_2O (Sigma, 99.9% D) as the buffered turnover solvent or 1.0 atm of C_2D_4 (Isotec, Inc., 99% D) using H_2O as the buffered turnover solvent. After initiation of turnover by the addition of Fe protein, the reaction was allowed to proceed for 30 min and quenched with 0.25 mL of 0.5 M EDTA-Na_2, pH 7.4. Headspace gas samples were extracted and analyzed by mass spectrometry (Hewlett-Packard GCMS, model 5971A) for the presence of C_2H_3D, $C_2H_2D_2$, and C_2HD_3. Headspace gas samples were similarly analyzed by Fourier transform infrared spectroscopy (FTIR) (MIDAC, model M2000) for the presence of C_2H_3D (946 cm^{-1}), *cis*- and *trans*-$C_2H_2D_2$ (843 and 988 cm^{-1}, respectively) and C_2HD_3 (943 cm^{-1}).

EPR and ENDOR Measurements: X-band EPR spectra were collected at 4K with a Bruker ER 300D spectrometer interfaced to a Bruker 1600 computer for data storage and collection. An Oxford Instruments ESR-900 helium flow cryostat positioned in a TE_{102} cavity was used to attain cryogenic temperatures. Continuous wave (CW) Q-band (35 GHz) EPR and ENDOR spectra were recorded at 2K in dispersion mode under "rapid-passage" conditions, as described elsewhere.[34] The bandwidth of the RF excitation was broadened to 100 kHz.[35] Q-band Mims pulsed ENDOR spectra were collected at 2K

(26) Yoo, S. J.; Angove, H. C.; Papaefthymiou, V.; Burgess, B. K.; Muenck, E. *J. Am. Chem. Soc.* **2000**, *122*, 4926−4936.
(27) Lovell, T.; Liu, T.; Case, D. A.; Noodleman, L. *J. Am. Chem. Soc.* **2003**, *125*, 8377−8383.
(28) Pickett, C. J.; Vincent, K. A.; Ibrahim, S. K.; Gormal, C. A.; Smith, B. E.; Best, S. P. *Chem.−Eur. J.* **2003**, *9*, 76−87.
(29) Thorneley, R. N. F.; Lowe, D. J. *JBIC, Journal of Biological Inorganic Chemistry* **1996**, *1*, 576−580.
(30) Lowe, D. J.; Fisher, K.; Thorneley, R. N. F. *Biochem. J.* **1990**, *272*, 621−625.
(31) Thorneley, R.; Lowe, D. *Biochem. J.* **1984**, *224*, 887.
(32) We shall ignore the possibility that some of those electrons reside on the P-cluster.
(33) Christiansen, J.; Goodwin, P. J.; Lanzilotta, W. N.; Seefeldt, L. C.; Dean, D. R. *Biochemistry* **1998**, *37*, 12611−12623.
(34) Werst, M. M.; Davoust, C. E.; Hoffman, B. M. *J. Am. Chem. Soc.* **1991**, *113*, 1533−1538.
(35) Hoffman, B. M.; DeRose, V. J.; Ong, J. L.; Davoust, C. E. *J. Magn. Res.* **1994**, *110*, 52−57.

with a spectrometer described previously.[36] The first-order ENDOR spectrum of a ^{1}H or ^{57}Fe nucleus, both with $I = {}^1/_2$, in a paramagnetic center is a doublet with frequencies given by[37]

$$\nu_{\pm} = |A/2 \pm \nu_N| \quad (1)$$

Here, ν_N is the nuclear Larmor frequency and A is the angle-dependent hyperfine coupling constant; here, the doublet is centered at $A/2$ and split by $2\nu_N$ when $\nu_N < A^N/2$ for N = ^{57}Fe, but it is centered at ν_N and split by A for N = ^{1}H. To obtain the principal values of the hyperfine tensors of the nuclei coupled to the electron spin center in the frozen-solution samples, 2-D datasets comprised of numerous ENDOR spectra collected across the EPR envelopes were analyzed as described elsewhere.[38−40]

Results

EPR: The resting state of the MoFe protein shows a well-defined rhombic EPR signal (**g** = [4.33, 3.77, 2.01]) arising from the lower Kramer's doublet ($m_s = \pm{}^1/_2$) of the $S = {}^3/_2$ FeMo-cofactor. Substitution of α-195^{His} by glutamine only slightly alters the resting-state cofactor EPR signal (**g** = [4.36, 3.64, 2.01]), implying the electronic structure of the cofactor remains essentially the same.[17] When the α-195^{Gln} MoFe protein turns over under C_2H_2, the EPR signal of the resting-state signal disappears and three new $S = {}^1/_2$ signals appear: **g** = [2.123, 1.978, 1.949] (S_{EPR1}); **g** = [2.007, 2.000, 1.992] (S_{EPR2}); and **g** = ∼1.972 (S_{EPR3}).[17,18] The S_{EPR1} signal comes from the FeMo-cofactor which has bound at least two C_2H_x-intermediate forms; S_{EPR2} is reassigned below; the S_{EPR3} signal is yet to be identified. The conversion of the cofactor S = 3/2 state to the S_{EPR1} (S = 1/2) state is comparable to the generation of $S = {}^1/_2$ signals when the wild-type MoFe protein turns over in the presence of CO and CS_2[14,16] but most especially to that during turnover with propargyl alcohol.[41] The S_{EPR1} state closely resembles the lo-CO cofactor (**g** = [2.09, 1.97, 1.93]), in which one CO molecule is bound. The electronic structures of the two $S = {}^1/_2$ cofactor states thus are expected to be similar.

Figure 3A compares the EPR spectrum of the ^{57}Fe-enriched α-195^{Gln} MoFe protein with that of the natural abundance protein incubated with C_2H_2 under turnover conditions. Both the S_{EPR1} and S_{EPR2} signals are broadened upon ^{57}Fe enrichment, confirming that both signals originate from the metalloclusters of the MoFe protein. In fact, the line-broadening of S_{EPR2} is rather surprising. Previously, S_{EPR2} was assigned to an amino acid or homocitrate radical produced during turnover of the altered MoFe protein in the presence of C_2H_2,[17] but the broadening identifies the $S = {}^1/_2$ S_{EPR2} state as metallocluster-related; detailed studies of S_{EPR2} are in progress. The broadening of the S_{EPR1} signal is expected because the signal originates from the FeMo-cofactor.[17,18]

^{57}Fe ENDOR: Figure 4 compares the "single crystal-like" ^{57}Fe ENDOR spectra obtained at the low- and high-field edges

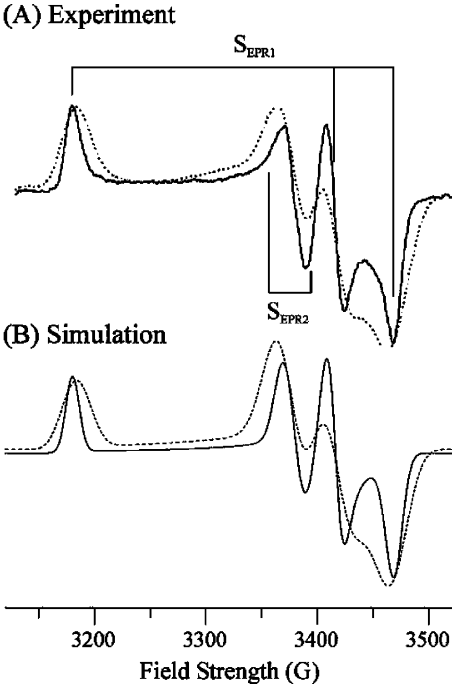

Figure 3. (A) X-band EPR spectra of naturally abundant (solid line) and ^{57}Fe-enriched (dotted line) α-195^{Gln} MoFe protein under turnover conditions with C_2H_2. (B) corresponding simulations, presented as the sum of simulated spectra for S_{EPR1} and S_{EPR2}. *Simulation parameters*: Natural-abundance (solid line) (S_{EPR1}) **g** = [2.123, 1.977, 1.947], LW (line width) = [12, 13, 15] G; (S_{EPR2}) **g** = [2.005, 1.998, 1.990], LW = [15, 15, 15] G. ^{57}Fe enriched (dotted line) for S_{EPR1} and S_{EPR2}, same g-tensors and LW as for natural abundance; for S_{EPR1}, seven ^{57}Fe with A_{iso} values presented in Table 1; for S_{EPR2}, an assumption of seven ^{57}Fe with A_{iso} = 25 MHz. *Experimental conditions*: microwave frequency, 9.45 GHz; microwave power, 5mW; modulation amplitude, 1 G; T = 2 K.

of the EPR envelopes of the ^{57}Fe-enriched α-195^{Gln} MoFe protein incubated with C_2H_2 (S_{EPR1}) and the ^{57}Fe-enriched MoFe incubated with CO under turnover conditions at low pressure of CO (lo-CO). In such a spectrum each magnetically distinct type of ^{57}Fe ($I = {}^1/_2$) gives a doublet centered at $A^{Fe}/2$ (depicted by "●") and split by twice the Larmor frequency ($2\nu_{Fe}$; "goal-posts") (eq 1).

The ^{57}Fe ENDOR signals of lo-CO were assigned as follows:[23] At the low-field edge (g_1) of the lo-CO signal (Figure 4A), three $\nu_{\pm}(^{57}Fe)$ doublets are identified with hyperfine couplings of $|\mathbf{A}|$ = 15 ($Fe_{\beta 1}$), 25 ($Fe_{\alpha 1}$), 37 ($Fe_{\alpha 2}$) MHz. The ν_- peak of the fourth site, $Fe_{\beta 2}$, is seen at ∼7 MHz with $|\mathbf{A}|$ = 19 MHz; its ν_+ partner is not explicitly identified. At the high-field edge (g_3) of lo-CO (Figure 4B), three Fe sites are seen with hyperfine couplings of $|\mathbf{A}|$ = 18 ($Fe_{\beta 1}$), 30 ($Fe_{\alpha 2}$), 34 ($Fe_{\alpha 1}$) MHz. The $Fe_{\beta 2}$ site is not well visualized because the bands overlap, but its presence is confirmed in spectra taken at other fields, as discussed presently.

The ^{57}Fe ENDOR signals of S_{EPR1} at g_1 are roughly comparable to, but less articulated than the corresponding signals from lo-CO (Figure 4A). At g_3, the ^{57}Fe ENDOR spectrum of S_{EPR1} is even more similar to, but still less resolved than that of lo-CO (Figure 4B). Both S_{EPR1} spectra can be assigned as four $\nu_{\pm}$ pairs from distinct types of Fe site. The four Fe pairs in the two spectra are temporarily denoted to "Fe_a" to "Fe_h" with the hyperfine couplings of $|\mathbf{A}|$ = 18 (Fe_a), 23 (Fe_b), 28 (Fe_c), 39 (Fe_d) MHz at g_1 and $|\mathbf{A}|$ = 17 (Fe_e), 21 (Fe_f), 31 (Fe_g), 33 (Fe_h) MHz at g_3. To correlate the $a-d$ signals with

(36) Davoust, C. E.; Doan, P. E.; Hoffman, B. M. *J. Magn. Reson.* **1996**, *119*, 38−44.
(37) Abragam, A.; Bleaney, B. *Electron Paramagnetic Resonance of Transition Ions*; Dover Publications: New York, 1986.
(38) Hoffman, B. M.; Venters, R. A.; Martinsen, J. *J. Magn. Res.* **1985**, *62*, 537−542.
(39) Hoffman, B. M.; DeRose, V. J.; Doan, P. E.; Gurbiel, R. J.; Houseman, A. L. P.; Telser, J. *Biol. Magn. Reson.* **1993**, *13(EMR of Paramagnetic Molecules)*, 151−218.
(40) Doan, P. E. In *Paramagnetic Resonance of Metallobiomolecules*; Telser, J., Ed.; American Chemical Society: 2003; pp 55−81.
(41) Benton, P. M. C.; Laryukhin, M.; Mayer, S. M.; Hoffman, B. M.; Dean, D. R.; Seefeldt, L. C. *Biochemistry* **2003**, *42*, 9102−9109.

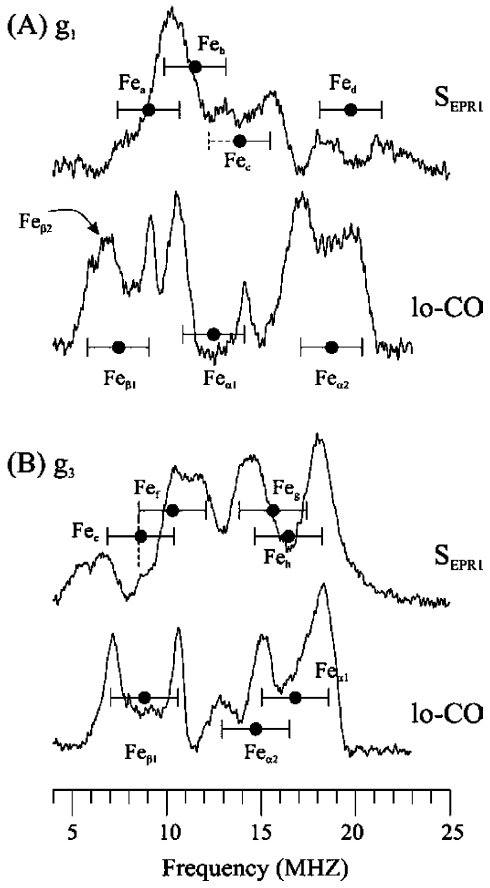

Figure 4. Q-band CW ^{57}Fe ENDOR spectra obtained at (A) the low-field edge, g_1, and (B) the high-field edge, g_3, of the EPR envelopes of the ^{57}Fe-enriched lo-CO and S_{EPR1} state MoFe proteins. The"goal posts" indicate ^{57}Fe doublets centered at $A_{Fe}/2$ (●). The spectra of lo-CO are adapted from ref 23. *Experimental conditions:* microwave frequency, (S_{EPR1}) 35.039 and (lo-CO) 35.160 GHz; modulation amplitude, (S_{EPR1}) 1.3 and (lo-CO) 0.7 G; g_1, (S_{EPR1}) 2.12 and (lo-CO) 2.09; g_3, (S_{EPR1}) 1.95 and (lo-CO) 1.93; RF power, 30 W; RF sweep speed, 1 MHz/s; $T = 2$ K.

the $e-h$ ones involves correlating ^{57}Fe ENDOR measurements across the EPR envelope of S_{EPR1} as was done in the case of lo-CO.[23]

Figure 5 presents such a 2-D field-frequency plot of ^{57}Fe ENDOR spectra for S_{EPR1}, along with the equivalent pattern for lo-CO. These 2D ^{57}Fe ENDOR patterns are strikingly similar. Both display a rich array of features from ~6 to ~22 MHz, corresponding to $15 \leq |\mathbf{A}| \leq 41$ MHz, and both can be interpreted in terms of four types of ^{57}Fe site. The ^{57}Fe hyperfine coupling tensors and valencies of the Fe sites of lo-CO were assigned previously and are summarized in Table 1.[23] The ^{57}Fe ENDOR features of S_{EPR1} can be assigned analogously. As indicated in Figure 5A, there are three distinct $\nu_\pm$ doublets, separated by $\sim 2\nu_{Fe}$, that run across the EPR envelope. These correspond to three iron sites, $Fe_{\beta 3}$, $Fe_{\alpha 3}$, and $Fe_{\alpha 4}$, whose assignments correlate the Fe_a, Fe_b, Fe_d doublets at g_1 with the Fe_e, Fe_h, Fe_g doublets at g_3, respectively (Figure 4). The hyperfine tensors obtained for these three sites are largely isotropic with $|\mathbf{A}_{iso}| = 32$ ($Fe_{\alpha 3}$), 33 ($Fe_{\alpha 4}$), and 18 ($Fe_{\beta 3}$) MHz (Table 1). A single ν_+ feature of a fourth site, labeled as $Fe_{\beta 4}$, is seen at ~16 MHz at g_1; the ν_- partner is not clearly seen under more intense peaks. However, at the high-field edge of the EPR envelope, g_3, the fourth site is seen as a doublet, labeled as $Fe_{\beta 4}$; the complete ENDOR pattern of this site cannot be followed across the EPR envelope because the intensity is low. We assign the fourth ^{57}Fe site at high- and low-field edges of the S_{EPR1} EPR envelope to the same Fe site, $Fe_{\beta 4}$; if each doublet belonged instead to a different Fe site, additional ENDOR features would be expected at g_1 and/or g_3. The $Fe_{\beta 4}$ site again has a largely isotropic hyperfine tensor, $|\mathbf{A}_{iso}| = 23-26$ MHz (Table 1).

Table 1. ^{57}Fe Isotropic Hyperfine Coupling Constants of ^{57}Fe-Enriched FeMo-cofactors of S_{EPR1} and lo-CO States[a]

^{57}Fe Site		S_{EPR1}		lo-CO	
valency	K/|K|[b]	site	$\mathbf{A}_{iso}$ (MHz)	site	$\mathbf{A}_{iso}$ (MHz)
$Fe^{+2.5}$	+	α_3	−32[c]	α_1	−30[g]
$Fe^{+2.5}$	+	α_4	−33[d]	α_2	−31[h]
Fe^{2+}	−	β_3	+18 (x4)[e]	β_1	+16 (x4)[i,j]
Fe^{2+}	+	β_4	−23 to −26[f]	β_2	~−17[j]

[a] Uncertainty in $\mathbf{A}_{iso}$, ±1 MHz unless noted. Signs of $\mathbf{A}_{iso}$ are not determined experimentally; rather they are deduced in the Discussion. [b] Signs of spin-projection coefficients. See eq 2. [c] $\mathbf{A} = -[29, 33, 33]$ MHz. [d] $\mathbf{A} = -[29, 31, 39]$ MHz. [e] $\mathbf{A} = +[16, 18, 20]$ MHz. (x4) indicates two spin-delocalized iron pairs. [f] $\mathbf{A} = -[21(1), 24.5 (3.5), 28(1)]$ MHz. [g] $\mathbf{A} = -[24, 31, 34]$ MHz. [h] $\mathbf{A} = -[26, 27, 39]$ MHz. [i] $\mathbf{A} = +[14, 15, 18]$ MHz. [j] The two ferrous Fe sites ($Fe_{\beta 1}$ and $Fe_{\beta 2}$) of lo-CO represent five Fe ions. One represents four Fe irons, and the other represents one Fe ion.

The ^{57}Fe patterns of $Fe_{\alpha 3}$ and $Fe_{\alpha 4}$ of S_{EPR1} are very like those of $Fe_{\alpha 1}$ and $Fe_{\alpha 2}$ of lo-CO, and the hyperfine tensors are similar (Table 1), implying that these sites have similar characteristics. Likewise, the behavior of $Fe_{\beta 3}$ of S_{EPR1} resembles that of $Fe_{\beta 1}$ (or $Fe_{\beta 2}$) of lo-CO, implying that these sites also correspond. However, the behavior of the $Fe_{\beta 4}$ site of S_{EPR1} with $|\mathbf{A}_{iso}| = 23-26$ MHz does deviate from that of the corresponding lo-CO. The same analysis which gave the signs of the hyperfine couplings for the four magnetically distinct ^{57}Fe sites of lo-CO yield the correspondences with the four magnetically distinct ^{57}Fe sites of S_{EPR1} presented in Table 1 and explained in the Supporting Information.

If inhibitor/substrate/product binding to the lo-CO and S_{EPR1} cofactor states were to cause one or more Fe ions to become intrinsically nonmagnetic (e.g., low-spin Fe^{2+}) or to have a negligible spin-coupling coefficient, then such an ion would exhibit substantially smaller hyperfine coupling than those associated with the signals in Figure 4. An example of the former case is given by the low-spin Fe^{2+} ($S = 0$) of Ni−Fe hydrogenase;[42] an example of the latter is given by the resting-state FeMo-co.[26] We were able to detect the 35 GHz Mims pulsed ENDOR signal from the hydrogenase Fe^{2+}: a doublet centered at $\nu_{Fe} \approx 1.7$ MHz and split by a coupling of $A \approx 1$ MHz (Figure S1).[42] We thus have made strenuous efforts with 35 GHz Mims pulsed and CW ENDOR to detect such signals from the ^{57}Fe lo-CO sample, as its EPR/ENDOR signal is more intense than that of S_{EPR1}. Such spectra of ^{57}Fe lo-CO collected at g_3 show *no* additional ^{57}Fe features beyond those seen for lo-CO in Figure 4A and, in particular, no doublet centered at ν_{Fe} (Figure S2A,B). Pulsed ENDOR studies of S_{EPR1} at g_3 also did not reveal additional low-frequency features (Figure S2C). Their absence for both turnover states is consistent with the inference that the ^{57}Fe signals of lo-CO and S_{EPR1} (Figure 4A) represent all seven ^{57}Fe of the cofactor. To test this, we have performed simulations of the S_{EPR1} EPR signal both with natural-abundance Fe and taking into account the ^{57}Fe line broadening

(42) Huyett, J. E.; Carepo, M.; Pamplona, A.; Franco, R.; Moura, I.; Moura, J. J. G.; Hoffman, B. M. *J. Am. Chem. Soc.* **1997**, *119*, 9291−9292.

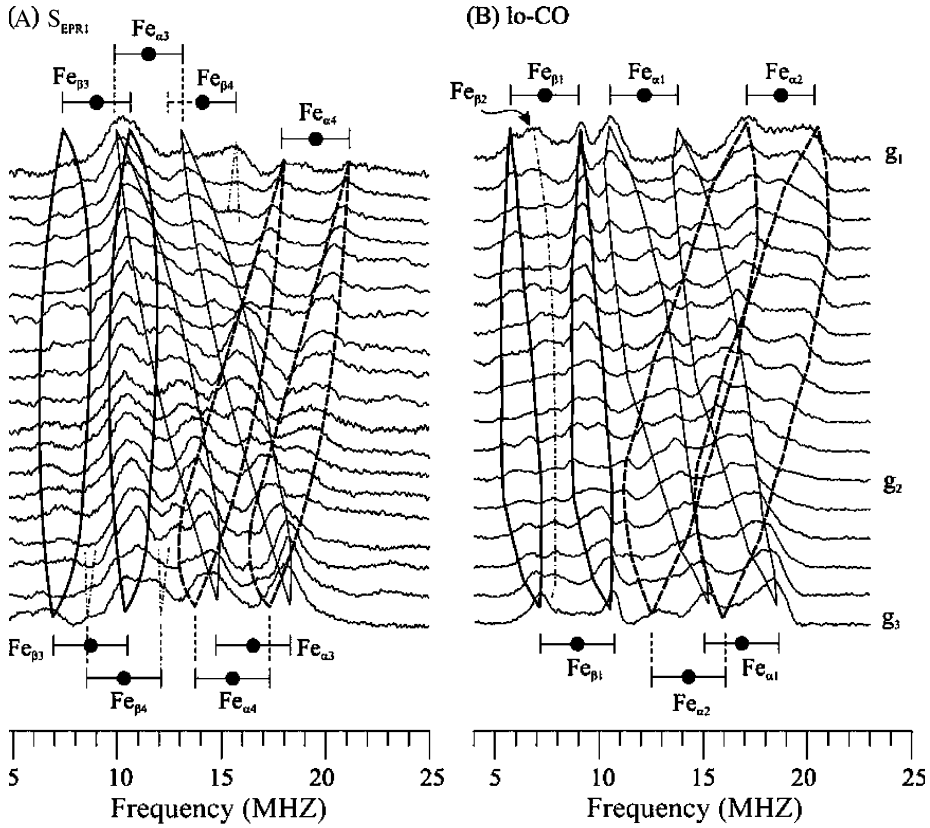

Figure 5. Q-band CW ^{57}Fe ENDOR spectra taken at fields across the EPR envelope of ^{57}Fe-enriched (A) S_{EPR1} and (B) lo-CO. The spectra of lo-CO are adapted from ref 23. The doublet patterns of the Fe sites are indicated by "goal-post" marks or an arrow, and their experimental variation with magnetic field is indicated. *Experimental conditions*, same as those in Figure 4.

using the hyperfine couplings derived by ENDOR (Table 1). Simulations which assumed that the four measured couplings represent seven ^{57}Fe ions are in reasonable agreement with experiment, Figure 3B; they are, however, only minimally better than simulations which assume each coupling represents a single ion, Figure S3.

^{1}H ENDOR: We had previously reported the presence of a broad, poorly resolved proton doublet with $A(^1H) \approx 12-14$ MHz in samples prepared with C_2H_2 in H_2O buffer and the absence of this signal in samples prepared with C_2D_2/D_2O.[18] An analogous result was subsequently reported for the turnover intermediate generated when the intermediate trapped during turnover of the α-70^{Ala} mutant with propargyl alcohol (PA); it shows a similar signal, but with a noticeably larger coupling, $A \approx 20$ MHz.[19] The resolved PA ^{1}H signal persists when either substrate or solvent is deuterated, showing that it has a contribution from equivalent hydrogenic species derived from substrate and from solvent. Quantitative ^{1,2}H ENDOR procedures, combined with the analysis of 2D field-frequency ENDOR patterns, showed that the two contributions have equal intensity and arise from two symmetry-equivalent protons bound to the C3 of a reduced form of PA. An additional signal was seen from a second *type* of proton that is solely derived from solvent and has a smaller coupling, $A \approx 6$ MHz. Analysis of these results disclosed that the product complex has the ferracycle structure pictured in Figure 2C.[19]

Our initial ^{1}H ENDOR study of S_{EPR1} trapped during turnover with acetylene found that the resolved ^{1}H signal persisted during turnover of C_2H_2 in D_2O buffer, but in apparent contrast to the PA intermediate it appeared to be lost during turnover with C_2D_2 in H_2O buffer. This finding implied that the C_2H_2 intermediate did not include a solvent-derived hydrogenic species and thus contained a complex of the acetylene reactant. However, S_{EPR1} accumulates to a lesser extent than does the PA turnover intermediate, gives weaker EPR and ENDOR signals than the PA intermediate, and the proton doublet in S_{EPR1} is less well-resolved.

In light of the results with PA, we have reexamined the S_{EPR1} intermediate prepared with the four combinations of protonated/deuterated substrate/solvent. Figure 6 presents ^{1}H ENDOR spectra collected at $g = 2.08$ from the S_{EPR1} intermediate formed during turnover of the α-195^{Gln} MoFe protein with $C_2^{1,2}H_2$ in buffers prepared with $^{1,2}H_2O$. Figure S4 presents 2D field-frequency plots of ^{1}H ENDOR spectra for these samples collected at multiple fields across their EPR envelopes. The spectra in Figures 6 and S4 show that the resolved 12−14-MHz-coupled ^{1}H signal seen for the C_2H_2/H_2O sample in fact persists in *both* the C_2H_2/D_2O and C_2D_2/H_2O samples and is eliminated only in the C_2D_2/D_2O sample. Thus, this proton signal is derived from both solvent *and* substrate and, hence, is associated with a product of acetylene reduction bound to the cofactor. The S_{EPR1} signals remain too weak to satisfactorily perform the quantitative ENDOR measurements needed to *prove* that the signals associated with the two sources are of comparable intensity, but in view of the results for the PA intermediate we take this to be the case. The signals from the two protons contributing to the strongly coupled signal are not resolved anywhere in the 2D field-frequency plots (Figure S4) and, thus, must have similar hyperfine tensors.

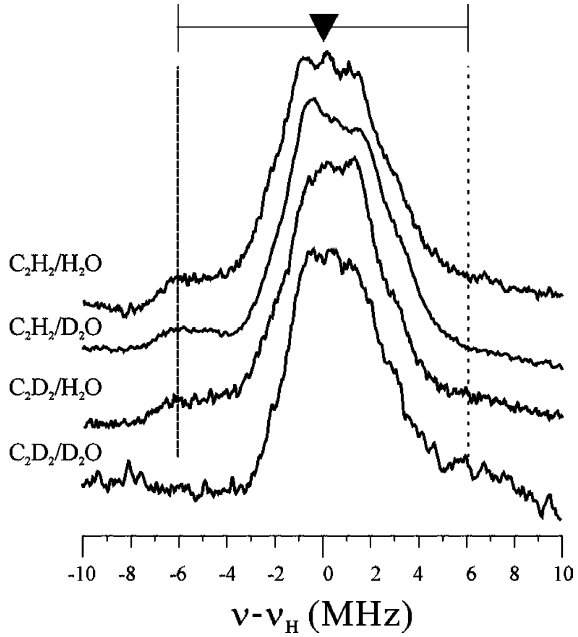

Figure 6. Q-band CW ^{1}H ENDOR spectra collected at $g = 2.08$ from S_{EPR1} prepared with the following isotopic compositions of substrate and buffer: C_2H_2/H_2O; C_2D_2/H_2O; C_2H_2/D_2O; C_2D_2/D_2O. *Conditions:* microwave frequency, 34.906−35.036 GHz; modulation amplitude, 4G; RF power, 20 W; RF sweep speed, 1 MHz/s; $T = 2$ K.

In the measurements of the PA turnover intermediate we also detected a signal from a second *type* of proton that is solely derived from solvent and has a smaller coupling, $A \approx 6$ MHz. Such a signal would be more difficult to detect in the ^{1}H spectra of the S_{EPR1} intermediate because the coupling to the resolved proton is smaller, and this would increase the overlap between the two if the second type was present. With that limitation, examination of the central portion of the^{1}H spectra of the several samples of S_{EPR1} did not disclose a second resolvable, exchangeable ^{1}H signal, Figure 6.

Turnover with C_2H_4: In an earlier paper,[17] we reported the surprising result that turnover with ethylene, the product of acetylene production, also induces the S_{EPR1} signal. Within our original model for S_{EPR1} as a substrate complex, this finding would require that the enzyme is able to deprotonate C_2H_4 and generate bound C_2H_2. If this were to occur, C_2H_4 should exhibit proton exchange with solvent. To test for this, nitrogenase turnover samples were prepared (see Materials and Methods) containing either C_2H_4 in D_2O or C_2D_4 in H_2O. Following 30 min of turnover, the headspace gas was tested for C_2H_3D, $C_2H_2D_2$, and C_2HD_3 using mass spectrometry and FTIR. No bands corresponding to any of the three isotopically exchanged compounds were detected with either technique.

Discussion

In this report we have presented new ^{1,2}H ENDOR evidence about the structure of the C_2H_2-derived species bound to the S_{EPR1} FeMo-cofactor and ^{57}Fe ENDOR evidence about the state of the S_{EPR1} cofactor itself. The two types of data, along with new mechanistic evidence, have been analyzed within a new formalism for the "electron inventory" of a turnover state. This has allowed us for the first time to correlate intermediates such as lo-CO and S_{EPR1} with the LT kinetic schemes for nitrogenase catalysis and further helps us refine our ideas of the structure of a bound species.

Nature of the C_2H_2-Derived Species Bound to the Cofactor of S_{EPR1}: We were led to reexamine the acetylene-derived species bound to the cofactor of S_{EPR1} in light of the more recent study of the intermediate trapped during turnover of the α-70^{Ala} MoFe protein with the larger alkyne, PA.[19] The PA intermediate is far more favorable for quantitative ENDOR investigation and analysis: it is trapped with a higher yield; its higher-intensity EPR/ENDOR signals allow the use of advanced, quantitative ENDOR techniques which fail with S_{EPR1}; the ^{13}C and ^{1}H ENDOR signals of the PA intermediate are better resolved than their counterparts in S_{EPR1}. However, with the studies of PA as a guide, we have collected additional ^{1}H ENDOR spectra from S_{EPR1} and reassessed this intermediate.

The ^{1}H and ^{13}C Q-band ENDOR studies of S_{EPR1} in this and the earlier report clearly indicate that it has an acetylene-derived moiety bound to the cofactor. The improved ^{1}H ENDOR data presented here confirm the presence of a single *type* of resolved proton signal with $A \approx 12-14$ MHz but also disclose that the signal persists in CW 35 GHz ENDOR spectra of *both* C_2D_2/H_2O and C_2H_2/D_2O samples; it disappears only in the C_2D_2/D_2O sample, as with the intermediate that forms during reduction of PA with the α-70^{Ala} MoFe protein. In conjunction with the earlier ^{13}C studies, this shows that the acetylene-derived moiety bound to the cofactor of S_{EPR1} contains hydrogens derived from both substrate and solvent and hence is a product of C_2H_2 reduction: C_2H_x, where $x = 3$ or 4.

The ^{13}C spectra of S_{EPR1} generated with $^{13}C_2H_2$ show three types of ^{13}C, requiring that no fewer than two molecules of C_2H_2, or its reaction intermediates/products, are associated with the S_{EPR1} FeMo-cofactor.[18] Two of these ^{13}C have similar hyperfine tensors, with isotropic couplings of essentially the same value: $a(C^1) \approx 2.5$ MHz; $a(C^2) \approx 2.3$ MHz. Both tensors appear to be roughly axial: that for C^2 is coaxial with **g** and has an anisotropic term, $2T(C^2) \approx 0.9$ MHz; that for C^1 has a somewhat larger anisotropic term, $2T(C^1) \approx 1.3$ MHz, and also is rotated from the **g**-tensor frame about g_2. The third carbon, $^{13}C^3$, has substantially weaker coupling.

There are two scenarios for explaining these findings. In Scenario I, the $^{13}C^1$ and $^{13}C^2$ with similar hyperfine couplings are assigned to a single C_2H_x species bound in a rather symmetrical manner to the cofactor, while the weakly coupled $^{13}C^3$ is assigned to a second acetylene-derived species; these are the assignments of our initial study. In this scenario, the presence of unresolvable signals from substrate and solvent-derived protons then suggests that S_{EPR1} contains a roughly symmetric final product, C_2H_4 ($x = 4$), rather than C_2H_3,with its intrinsically inequivalent $-CH_2$ and $-CH$ "halves". Similar interactions of the two ^{13}C with the cluster is not likely if C_2H_4 bridges two Fe ions across a 4-Fe face (Figure 2B).[43] Even though such a structure might be roughly *geometrically* symmetric, in general the two Fe ions would not have the same cluster spin-coupling coefficients, and hence the hyperfine couplings to the two ^{13}C would be quite different. The hyperfine tensor for a ^{13}C interacting with Fe^i ($^{13}C^i$) has the form of eq 2,[44,45]

$$\mathbf{A}_{exp}(^{13}C^i) = K(Fe^i)\mathbf{A}(^{13}C^i)^u \qquad (2)$$

where $K(Fe^i)$ is the spin-projection coefficient of the *i*-th Fe site and $\mathbf{A}(^{13}C^i)^u$ is the hyperfine constant for the ^{13}C interacting

with the uncoupled Fe^i; an analogous equation holds for ^1H.[46] According to eq 2, for the two ^{13}C of a C_2 fragment to have comparable hyperfine coupling tensors, not only must the $\mathbf{A}(^{13}C^i)^u$ be comparable but also so must the $K(Fe^i)$, and this seems unlikely to us.[47]

In fact, the absence of proton exchange between ethylene and solvent during enzymatic turnover in the presence of C_2H_4 in D_2O or C_2D_4 in H_2O is the best evidence that S_{EPR1} contains bound C_2H_4 and not the acetylene reactant or a singly reduced intermediate. In either of the latter two cases, there would be proton exchange with solvent.

In Scenario I, analogy to the results for the PA intermediate makes it reasonable to propose that the ethylene of S_{EPR1} is bound to a single Fe as a ferracycle, Figure 2C, presumably with Fe6 as the site of binding.[19,20,48] The breadth of the ^1H ENDOR signals of S_{EPR1}, which likely reflects unresolved differences in ^1H coupling to the protons on the two halves of the C_2H_4, precludes the detailed ^1H ENDOR study that would confirm this. In this scenario, the weakly coupled $^{13}C^3$ might be associated with a nearby C_2H_2 waiting "in the queue".

In an alternate Scenario II, one would assign $^{13}C^1$ and $^{13}C^2$ to two slightly *different* acetylene-derived C_2H_x species bound to the cofactor; each could represent one relatively strongly coupled carbon of an unsymmetric species, or the two carbons of a symmetric one. $^{13}C^3$ then would be assigned to the other half of one or both of the unsymmetric bound species or (unlikely) a third species.

However, formulation of Scenario II in terms of two C_2H_3 ($x = 3$) also is contradicted by the absence of detectable exchange during turnover of C_2H_4 in D_2O or C_2D_4 in H_2O (*see above*). This leaves as a Scenario II possibility the presence of *two* C_2H_4 bound to the cofactor in a highly unsymmetric fashion. We do *not* favor this scenario, as follows. The similarity of the ^{57}Fe ENDOR data for S_{EPR1} and for lo-CO, which binds a single CO, suggests that S_{EPR1} correspondingly binds a single C_2H_4. Likewise, analogy to the PA intermediate, which binds one alkene, suggests the same would be true for S_{EPR1}. Most important, this scenario would require that a "second" C_2H_2 binds to the cofactor and is reduced to bound C_2H_4 before the "first" C_2H_4 is released, contrary to the finding by Lowe et al.[30] that the C_2H_4 product is released before the next C_2H_2 substrate binds. Thus, we favor Scenario I, with its single bound C_2H_4.

Binding Sites of C_2H_4 and CO: Our previous ^{13}C and $^{1,2}H$ ENDOR studies of lo-CO suggested that CO bridges two Fe ions of a 4-Fe cofactor face (Figure 2A),[14] and we here propose that S_{EPR1} contains C_2H_4 bound to one Fe ion of such a face, most likely Fe6 of the Fe-2,3,6,7 face. Following these suggestions, there are two types of model for the relative binding sites of CO and C_2H_4, Figure 7: both molecules bound to the same face, with one Fe site in common, as in Figure 7A; the two molecules bound independently, possibly but not necessarily on the same face as in Figure 7B.

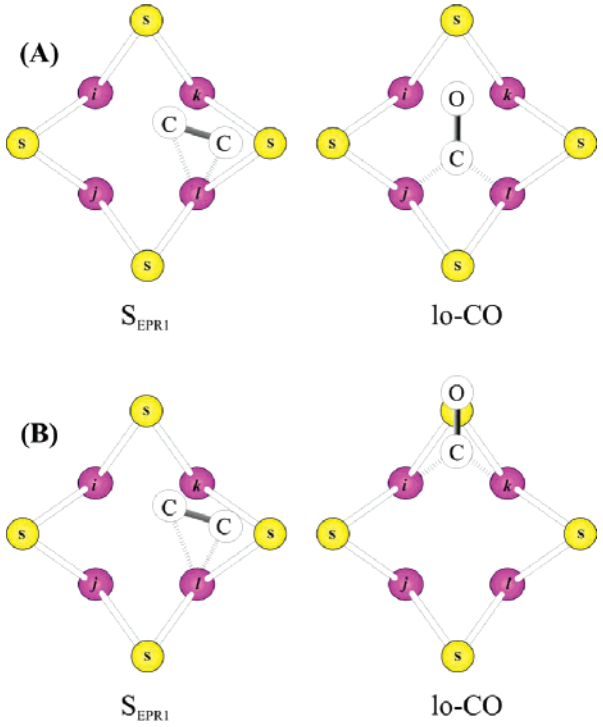

Figure 7. Two possible relative binding modes of CO to the lo-CO FeMo-cofactor and C_2H_2 to the S_{EPR1} FeMo-cofactor.

We can distinguish between these two alternatives if we recognize the essential similarities of the cofactor states in lo-CO and S_{EPR1}. The *g* values of the two intermediates are essentially the same, suggesting a common electronic state: $\mathbf{g}$(lo-CO) = [2.09, 1.97, 1.93]; $\mathbf{g}(S_{EPR1})$ = [2.123, 1.978, 1.949]. The ^{57}Fe ENDOR measurements show that only one ^{57}Fe hyperfine coupling differs within error between lo-CO and S_{EPR1}, the unique ferrous ion, $Fe_{\beta 4}$ of S_{EPR1} vs $Fe_{\beta 2}$ (or $Fe_{\beta 1}$) of lo-CO (Table 1). These basic similarities imply that the cofactors of the two intermediates share a common electronic state, with similar electronic structures and spin-coupling, and thus similar spin-projection coefficients. It thus seems plausible that the change of ^{57}Fe hyperfine coupling of the unique ferrous site largely reflects a difference in coordination of substrate/inhibitor.

The observation of such a difference in a single Fe signal suggests that CO and C_2H_4 do not occupy disjoint sites. For a situation such as that in Figure 7B, there would likely be three Fe ions with substantially different couplings in the two intermediates. The data instead favors a common Fe ion, such as Figure 7A, where only Fe *j* would likely show a major change, as it binds an exogenous ligand in lo-CO, but none in S_{EPR1}. We note that the proposed modes of binding CO and C_2H_2 to Fe ions on the same face, with one common Fe ion, are compatible with the mechanistic conclusions that the two bind to different "sites" and that CO is a noncompetitive inhibitor of C_2H_2 reduction.[29−31,49−51]

Cofactor Valencies of lo-CO, S_{EPR1}, and Resting States: The valencies of the cofactor ions of lo-CO were assigned previously from ^{57}Fe ENDOR measurements.[23] We proposed that the four observed ^{57}Fe classes of lo-CO represent all seven

(43) It is even less likely for a bridge between Fe and Mo.
(44) Noodleman, L.; Peng, C. Y.; Case, D. A.; Mouesca, J. M. *Coord. Chem. Rev.* **1995**, *144*, 199−244.
(45) Mouesca, J. M.; Noodleman, L.; Case, D. A.; Lamotte, B. *Inorg. Chem.* **1995**, *34*, 4347−4359.
(46) For bridging species, eq 2 must be summed over interacting Fe.
(47) We think an "accidental" equality of the products when the individual factors are different to be even more unlikely.
(48) Igarashi, R. Y.; Dos Santos, P. C.; Niehaus, W. G.; Dance, I. G.; Dean, D. R.; Seefeldt, L. C. *J. Biol. Chem.* **2004**, *279*, 34770−34775.
(49) We further suggest below that the two intermediates represent different LT kinetic states.
(50) Shen, J.; Dean, D. R.; Newton, W. E. *Biochemistry* **1997**, *36*, 4884−4894.
(51) Han, J.; Newton, W. E. *Biochemistry* **2004**, *43*, 2947−2956.

Fe sites in the FeMo-cofactor: $Fe_{\alpha 1}$ and $Fe_{\alpha 2}$ form a mixed-valence pair ($2Fe^{2.5+}$) in which an Fe^{3+} and an Fe^{2+} ion have one electron (hole) delocalized between them; $Fe_{\beta 1}$ and $Fe_{\beta 2}$ constitute the remaining five Fe^{2+} sites of the cofactor. This assignment implicitly assumes that the spin-coupling scheme for the $S = {}^1/_2$ cofactor state is like those of $[Fe_4S_4]$ clusters, involving high-spin ions that do not exhibit small spin-coupling coefficients and correspondingly small observed couplings. The absence of weakly coupled ^{57}Fe signals in the 35 GHz Mims ^{57}Fe pulsed ENDOR measurements described here (Figure S2) (plus the slight improvement in simulations of the ^{57}Fe line broadening of the EPR spectrum through use of the ENDOR-derived hyperfine couplings for the seven ^{57}Fe of the cofactor rather than four (Figure S3)) adds some support to this assumption; it will be tested further with W-band ^{57}Fe ENDOR measurements.

The ^{57}Fe ENDOR analysis for lo-CO, combined with an assigned Mo^{4+} oxidation state, unchanged from that of the resting-state,[52] implied a valency and electron count for the FeMo-cofactor in lo-CO of $[Mo^{4+}, Fe^{3+}, Fe^{2+}{}_6, S^{2-}{}_9]^{+1}(d^{43})$; the same assignment was made for hi-CO. Because the resting state can be recovered from lo-CO merely by pumping off the CO without addition of oxidant or reductant, we further assigned these valencies and electron count to the resting state. Smith and co-workers have since suggested that lo-CO is in fact doubly reduced relative to the resting state and that when the CO is pumped off, the lo-CO cofactor two protons are reduced to H_2, thereby restoring the resting state.[28] We accept this suggestion as the appropriate way to connect our study of the intermediate with Mössbauer experiments[26] and DFT computations[27,53−56] which suggested that the $S = {}^3/_2$ resting-state cofactor (*Av1*) has the electronic state, $[Mo^{4+}, Fe^{3+}{}_3, Fe^{2+}{}_4, S^{2-}{}_9]^{3+}$ (d^{41}). In support of these conclusions, an FTIR spectroelectrochemical study of the isolated FeMo-cofactor from *Kp* nitrogenase under CO atmosphere[57] suggested that the CO-bound cofactor states can be achieved at the one- or two-electron reduced level beyond the resting state in binding geometries consistent with our suggestions based on the ^{13}CO ENDOR studies (Figure 2A).

We have employed the same protocol developed for interpreting ^{57}Fe ENDOR of the lo-CO cofactor to that of S_{EPR1}. It characterizes the ^{57}Fe hyperfine couplings of an ion in terms of its observed isotropic hyperfine coupling constant and a parameter, a_{test}, which is the weighted average of the intrinsic isotropic constants for all Fe sites.[45] The ^{57}Fe ENDOR measurements on S_{EPR1} reported here show a 1:1 correspondence between the ^{57}Fe ENDOR signals of lo-CO and S_{EPR1}, Table 1. The analyses for lo-CO and S_{EPR1} are virtually the same, and indicate that the cofactors of the two share the electronic state, $[Mo^{4+}, Fe^{3+}, Fe^{2+}{}_6, S^{2-}{}_9]^{+1}(d^{43})$, reduced by $m = 2$ electrons relative to the resting state.

Electron Inventory and E_n States of Intermediates; Application to lo-CO: To correlate nitrogenase turnover intermediates with the LT kinetic schemes for substrate reduction, we introduce the concept of an "electron inventory", which relates the number of electrons a MoFe protein intermediate has accepted from the Fe protein (n) to the number which have been transmitted to the substrate (s), the number that reside on the intermediate cofactor in excess of those on the resting state cofactor (m), and the number delivered to the cofactor from the P clusters of this intermediate (p): $n = m + s - p$.

As the first application of the electron inventory formalism, consider the simple case of lo-CO. First, as CO does not bind to the resting state, it must bind to a reduced form of the enzyme, an LT E_n state with $n > 0$. The FeMo-co of lo-CO is doubly reduced, $m = 2$, relative to the resting state (see above). When CO binds to a metal ion or ions, it usually does so through dative bonding, without being reduced. CO binding to the cofactor of lo-CO is no exception, as shown by the high C−O stretching frequencies of bound CO.[57] Thus, $s = 0$ for the cofactor-bound CO. As we have never seen EPR signals from any intermediate that can be assigned to an oxidized P cluster,[58,59] we may take $p = 0$ for lo-CO, giving $n = m + s - p = 2 + 0 - 0 = 2$: lo-CO is an E_2 kinetic state; we denote its cofactor, which is doubly reduced relative to the M^N resting state, as M^{N-2}. Below, we drop p from the equations as applied to lo-CO and S_{EPR1}.

E_n State and Ethylene Binding Geometry of S_{EPR1}: The ^{57}Fe ENDOR measurements on S_{EPR1} reported here indicate that the cofactor of this intermediate, like that of lo-CO, is 2-fold reduced relative to the resting state: $m = 2$. We conclude above that S_{EPR1} incorporates a complex of the ethylene product bound to the cofactor, as in the case of the allyl alcohol complex formed during turnover of propargyl alcohol. Thus, in these cases, no fewer than $s = 2$ of the n electrons transferred to the MoFe protein must have been "transmitted" (along with the addition of two protons) to the alkyne ("C_2R_2") substrate during the reductive formation of two C−H bonds. Thus, $n \geq 4$ electrons have been delivered to the MoFe protein of S_{EPR1}. If the alkene binds to a cofactor Fe as a dative π-donor, Figure 8, analogously to the dative bonding of CO, then[60] the binding does not alter the valency of the cofactor. As a result such a product complex of alkyne reduction has an electron inventory, $n = m + s = 2 + 2 = 4$: while lo-CO is an E_2 state, S_{EPR1} with a dative C_2H_4 would be an E_4 state. The cofactor reduction level and bonding can be denoted, M^{N-2}-[π-(C_2H_4)].

One might also imagine that $C_2R_2H_2$ actually binds by C−Fe σ-bonds, as the ferracyclopropane we had originally drawn for convenience in the PA study, Figure 8; such a structure would occur upon oxidative addition of a $C_2R_2H_2$ moiety to the $M^{N-(n-2)}$ cofactor and would be recognizable by the bond angles around the C_2 carbons. In this case the alkene must be considered to have accepted two additional electrons from the cofactor, making a total of $s = 4$ electrons transferred to the C_2H_2 substrate; in the highly reduced polynuclear FeMo-co, electron redistribution within the cluster would surely prevent the formation of a high-valent Fe ion at the binding site.[61]

(52) Venters, R. A.; Nelson, M. J.; McLean, P. A.; True, A. E.; Levy, M. A.; Hoffman, B. M.; Orme-Johnson, W. H. *J. Am. Chem. Soc.* **1986**, *108*, 3487−3498.
(53) Dance, I. *Chem. Commun.* **2003**, *3*, 324−325.
(54) Hinnemann, B.; Norskov, J. K. *J. Am. Chem. Soc.* **2003**, *125*, 1466−1467.
(55) Durrant, M. C. *Biochemistry* **2004**, *43*, 6030−6042.
(56) Vrajmasu, V.; Muenck, E.; Bominaar, E. L. *Inorg. Chem.* **2003**, *42*, 5974−5988.
(57) George, S. J.; Ashby, G. A.; Wharton, C. W.; Thorneley, R. N. F. *J. Am. Chem. Soc.* **1997**, *119*, 6450−6451.
(58) Tittsworth, R. C.; Hales, B. J. *Biochemistry* **1996**, *35*, 479−487.
(59) Hagen, W. R.; Wassink, H.; Eady, R. R.; Smith, B. E.; Haaker, H. *Eur. J. Biochem.* **1987**, *169*, 457−465.
(60) This is so regardless of whether the cofactor Fe ion(s) remain in the high-spin state with C_2H_4 bound or convert to intermediate- or low-spin.
(61) Such a valency assessment has no consequences for the magnetism of a "typical" organometallic center, with $S = 0$ even-electron metal ions. However, in principle it has experimentally observable consequences for the magnetic properties of a metal cluster comprised of spin-coupled high-spin, open-shell Fe(II/III) ions: the two electrons provided by the cofactor

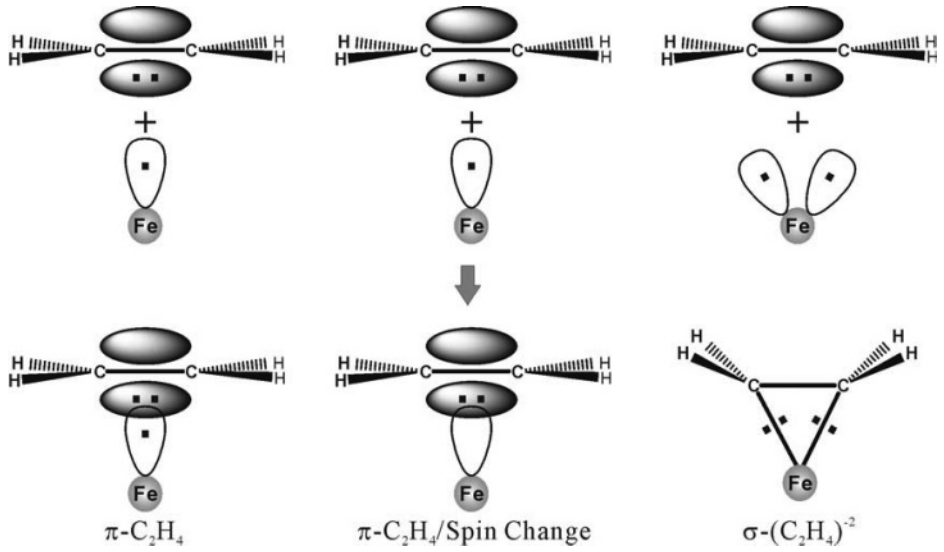

Figure 8. Cartoon representation of alternate schemes for binding C_2H_4 to a cofactor high-spin metal ion. (Left) Dative π bonding without change in metal-ion spin state. (Middle) Dative π bonding with spin-pairing to yield intermediate- or low-spin metal ion; the other unpaired electron (top) and the new spin pair (bottom) are not shown. (Right) Oxidative addition to form Fe−C σ bonds.

Table 2. Electron Inventory of Nitrogenase MoFe Protein States

cofactor	resting state	lo-CO	S_{EPR1} π-$C_2R_2H_2$	S_{EPR1} σ-$(C_2R_2H_2)^{-2}$
spin	$^3/_2$	$^1/_2$	$^1/_2$	
E_n state[a]	E_0	E_2	E_4	E_6
m[b]	0	2	2	2
s[c]	0	0	2	4
d-electron count[d]	d^{41}	d^{43}	d^{43}	d^{43}

[a] $n = m + s$. [b] Cofactor reduction level. [c] Substrate reduction level. [d] $(d^{41}) = [Mo^{4+}, Fe^{3+}{}_3, Fe^{2+}{}_4, S^{2-}{}_9]^{+3}$, $(d^{43}) = [Mo^{4+}, Fe^{3+}{}_1, Fe^{2+}{}_6, S^{2-}{}_9]^{+1}$.

Combining the conclusion that the lo-CO and S_{EPR1} cofactors both are doubly reduced relative to the resting cofactor ($m = 2$) with the deduction that $s = 4$ when a bound alkene forms a σ-bonded ferracyclopropane species, Figure 8, then adoption of such a bonding mode would imply that $n = m + s = 2 + 4 = 6$, namely that S_{EPR1} is E_6 (Table 2).

The ^{1,2}H and ^{13}C ENDOR of the S_{EPR1} intermediate is too poorly resolved to offer hope that the discrimination between dative and σ-binding modes can be achieved experimentally,[62] but we can apply the above framework to choose the appropriate electron inventory and make inferences about the ethylene bonding geometry for the S_{EPR1} intermediate, as follows. Lowe et al. found that C_2H_4 is released from the E_3 and E_4 states during C_2H_2 reduction by WT enzyme.[30] S_{EPR1} does not accumulate in the WT enzyme, so in this case either E_4 promptly releases C_2H_4 or the WT enzyme does not reach E_4 and releases the product at the EPR-silent E_3 state, yielding the E_1 state (also EPR-silent),

$$E_3(\pi\text{-}C_2H_4) \rightarrow C_2H_4 + E_1$$

which cannot generate H_2 without addition of another electron. Now let us imagine that the EPR-active S_{EPR1} intermediate which accumulates with the α-195^{Gln} MoFe protein is an E_4 state (Figure 9) that has been stabilized by the mutation, with $m = 2$ electrons residing on the cofactor and $s = 2$ on the substrate. When C_2H_4 is released the enzyme would be in E_2; the M^{N-2} cofactor could bind another C_2H_2 substrate, but also it could give off H_2 and return the enzyme to E_0 (Figure 9),[30]

$$E_4(\pi\text{-}C_2H_4) + 2H^+ \rightarrow C_2H_4 + H_2 + E_0$$

Such production of H_2 during C_2H_2 reduction would make the α-195^{Gln} MoFe protein less efficient at C_2H_2 reduction than the WT protein, which is exactly what Newton and co-workers found:[25] even though both the WT and α-195^{Gln} MoFe proteins have identical K_m for acetylene reduction, the α-195^{Gln} MoFe protein has a smaller electron allocation into ethylene production than the WT protein. Furthermore, if S_{EPR1} were a trapped E_6 state, it is likely that the bound ethylene would in part undergo further reduction to ethane, most likely with generation of H_2 and return to resting state,

$$E_6(\sigma\text{-}C_2H_4) + 4H^+ \rightarrow C_2H_6 + H_2 + E_0$$

However, no ethane is detected during C_2H_2 reduction by the α-195^{Gln} MoFe protein.[24,25] We therefore conclude that S_{EPR1} is an E_4 state (Figure 9) in which the product, C_2H_4, binds as a π-donor in the ferracycle of Figure 8 and Figure 2C; at present we cannot infer the effects of C_2H_4 binding on the spin state of the Fe to which it binds (Figure 8).

Conclusions

We have reexamined ^{1}H ENDOR of S_{EPR1} MoFe protein with C_2H_2/C_2D_2 in H_2O/D_2O buffers in light of our recent discovery that the product, allyl alcohol, is trapped during reduction of PA by the α-70^{Ala} MoFe protein.[19] This has shown that S_{EPR1} in fact binds C_2H_4, the reduction product of C_2H_2, a result confirmed by the absence of H/D exchange with solvent during turnover with C_2H_4. We further suggest that the C_2H_4 binds to a single Fe of the cofactor as a ferracycle, as proposed for allyl alcohol.

The ^{57}Fe ENDOR measurements of the ^{57}Fe-enriched S_{EPR1} FeMo-cofactor (Figure 5A) disclose a one-to-one correspondence of the sites in the S_{EPR1} and lo-CO cofactors (Table 1),

to the C−Fe σ-bonds of the ferracyclopropane no longer participate in the cluster spin system, and the consequence to the ion would be the same (magnetically) as if complex formation had driven it to intermediate spin.

(62) The same may not be true for bound allyl alcohol.

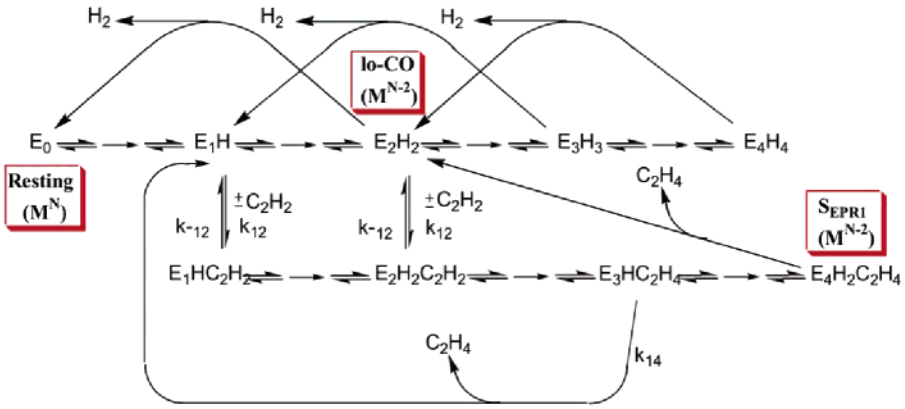

Figure 9. Kinetic scheme for C_2H_2 binding and reduction by nitrogenase as adopted from Lowe et al.[30] to show the placement of resting, lo-CO, and S_{EPR1} states within the scheme.

indicating that electronic structures and magnetic couplings of the two states are similar and are describable with the valency model proposed in the previous ^{57}Fe ENDOR study of lo-CO: $[Mo^{4+}, Fe^{3+}, Fe_6^{2+}, S_9^{2-}(d^{43})]^{+1}$. Following the suggestion of Smith and co-workers, this state is doubly reduced (reduction level, M^{N-2}) relative to the M^N (d^{41}) resting-state cofactor.[28] Only one ^{57}Fe hyperfine coupling differs appreciably in S_{EPR1} and lo-CO. This suggests a picture in which a bridging CO of lo-CO and the C_2H_4 of S_{EPR1} share a common Fe site, as in Figure 7A; in such cases only site *j* would likely show a major change, as it binds an exogenous ligand in lo-CO, but none in S_{EPR1}.

To correlate turnover intermediates with kinetic schemes for substrate reduction we have introduced the concept of an "electron inventory". It relates the number of electrons an MoFe protein intermediate has accepted from the Fe protein (n) to the number which have been transmitted to the substrate (s), the number that reside on the cofactor (m), and the number delivered to the cofactor from the P clusters (p): $n = m + s - p$ (with $p = 0$ here). We have applied this formalism to the two intermediates discussed here, showing how an electron inventory can be determined by combining ENDOR data with results from studies of catalysis. The lo-CO intermediate has an $m = 2$ (doubly reduced) cofactor, $s = 0$ electrons delivered to bound CO, and thus $n = m + s = 2$: lo-CO is an E_2 kinetic state of the MoFe protein, Figure 9. The S_{EPR1} intermediate also has an $m = 2$ (M^{N-2}) cofactor, but at least $s = 2$ electrons (plus two protons) have been delivered to the substrate to form the bound C_2H_4 product, so in this case $n = m + s \geq 4$. Consideration of the catalytic efficiency of the α-195^{Gln} MoFe protein leads us to conclude that S_{EPR1} is an E_4 kinetic state (Figure 9) in which the doubly reduced cofactor ($m = 2$) binds the C_2H_4 ($s = 2$) product through dative π bonding (Figure 8).

While the Lowe−Thorneley scheme of nitrogen fixation clearly specifies the kinetic relation between E_n states during the reduction of various substrates, the characterization of any of those states has, until now, eluded investigators. This paper identifies, for the first time, the substrate binding and the reduction states of both the FeMo-cofactor and the substrate of an E_n mechanistic intermediate during enzyme turnover.

Acknowledgment. This work has been supported by the NSF (MCB-0316038, B.M.H.), the USDA (2003-02105 NRI, CSREES, B.J.H.), the Korea Research Foundation (KRF-2003-070-C00029, H.-I.L.), and the NIH (GM59087, D.R.D.; HL 13531, B.M.H.). We thank Dr. Joshua Telser, Roosevelt University, for extraordinarily helpful comments.

Supporting Information Available: Text plus three figures. This material is available free of charge via the Internet at http://pubs.acs.org.

JA054078X